Does Ocean Turbulence Peak at the Equator?: Revisited

D. HEBERT, J. N. MOUM, AND D. R. CALDWELL

College of Oceanography, Oregon State University, Corvallis, Oregon

31 January 1991 and 15 April 1991

ABSTRACT

In spite of the effects of several forms of temporal variability that tend to mask geographical patterns in turbulence intensity, our evidence indicates that the turbulence is enhanced above the equatorial undercurrent in comparison to latitudes north and south of it. This evidence consists of three meridional transects of microstructure observations across the equator (at 140°W in 1984 and 1987, and at 110°W in 1987) along with an equatorial station at 140°W and a longitudinal transect along the equator from 140°W to 110°W. All three meridional transects show a peak in averaged estimates of the turbulent kinetic energy dissipation rates, ϵ, at the equator, although in 1984 the peak was not significant at the 95% level. The major sources of temporal variability were the diurnal buoyancy flux variation and the wind stress variations, which had a typical period of a few days. After the diurnal variability is removed by averaging, it can be shown that, for similar wind stress, ϵ is larger over the undercurrent than away from it. Examination of the 16-m, 1-hour averaged ϵ, in terms of the vertical shear of horizontal velocity and the stratification (determined over similar space and time scales), indicated a tendency of this mean ϵ to vary with the Richardson number, Ri, when Ri < 1. However, closer examination showed that the dependence of ϵ on Ri varied with depth. Therefore, a simple parameterization for mixing rates on Ri is not valid for all depths.

1. Introduction

Several attempts have been made over the past few years to settle the question of whether the vertical shear associated with equatorial currents causes an equatorial peak in meridional sections of turbulence measurements. Such a peak is hypothesized because of the experimental and theoretical evidence that sheared stratified flows become unstable when the Richardson number decreases to a value lower than a critical Richardson number Ri_c, usually 0.25 (Turner 1973). (The Richardson number, Ri, is defined as N^2S^{-2}, N being the buoyancy frequency, taken as a measure of the stabilizing influence by the vertical stratification, and S being the shear, a measure of destabilization.) The instabilities produced at low values of Ri tend to cause turbulence and thereby vertical mixing in the water column. Therefore, we might expect more intense turbulence, quantified as large values of the rate of dissipation of kinetic energy, ϵ, in regions of low Ri.

Values of Ri lower than usual in the ocean thermocline are found in the equatorial Pacific between the core of the eastward-flowing equatorial undercurrent (EUC) located in the thermocline and the usually westward-flowing surface layer. A large mean shear is usually present so that, even though the stratification is significant, the value of Ri is usually estimated to be less than 0.5, even when Ri is estimated over vertical scales as large as 16 m and time scales as long as hours or days.

We envision the large-scale mean Ri being maintained at a low value by the mean shear and the vertical shear produced by smaller scale features such as high-frequency internal waves locally reducing Ri_c even more, to a value less than Ri_c, thereby producing turbulent events (Moum et al. 1991). In the more common oceanic situation, away from mean shear, it is less likely that the vertical shear produced by the smaller scale features can reduce the Ri to a value less than Ri_c. By this reasoning, in a meridional section, we would expect a peak in ϵ over the EUC.

Attempts to confirm this hypothesis have produced mixed results. An early attempt seemed to indicate a peak narrower than expected (Crawford and Osborn 1981; Crawford 1982). Moum et al. (1986b) found no peak and surprisingly large time variability. Results from a 1984 two-ship expedition showed mixed results; Peters et al. (1989) found a peak, but Moum et al. (1986a) did not.

Why the seemingly contradictory results? The contradiction is probably caused by a combination of unexpected variability and limited sampling schemes. Crawford's (1982) data were all taken during daylight hours, with peak values being found in a period following high winds. Moum et al.'s (1986b) measurements were all made at night. Peters et al.'s (1989)

Corresponding author address: Dr. Dave Hebert, College of Oceanography, Oregon State University, Ocean Admin. Bldg. 104, Corvallis, OR 97331-5503.

1984 measurements, consisting of bursts of several hours' sampling at a fixed location, were made during four cross-equatorial transects. The 1984 measurements of Moum et al. (1986a) were made in a single cross-equatorial transect and a 12-day time series on the equator, done on a continuous 24-hour a day basis, but even with this dataset, the separation of temporal from spatial variations presents a challenge in analysis.

What are the major sources of temporal variability? On a time scale of several days (the time it takes a ship to make a transect across the EUC), two major sources of variability have been identified to date. In 1984 an extraordinary diurnal variation in turbulence intensity was found (Gregg et al. 1985; Moum and Caldwell 1985). For example, the average value of ϵ in the region of large shear below the mixed layer (e.g., at 55 m) was 100 times larger at midnight than it was at noon (Moum et al. 1989). (The results of later cruises indicate that this exceptional diurnal variability is seen only in periods of fairly high winds.) Also in 1984, evidence of a strong dependence of the intensity of turbulence in the thermocline on the surface wind stress was observed (Moum and Caldwell 1985). Although more recent data show a larger scatter than the original observations, there is little doubt that the local wind stress has a critical effect on thermocline turbulence. At this location, the wind stress can vary quite significantly in only a day or two.

Sampling schemes intended to demonstrate the existence of a meridional peak in the turbulence intensity have to be evaluated against the possibility of confusing temporal variations caused by these other influences with the hypothesized geographical pattern. To reduce the effect of surface influences, Peters et al. (1989), for example, used a different depth averaging than Crawford (1982). Crawford had plotted a depth-integrated (15–110 m) estimate of ϵ. Peters et al. (1989) eliminated the mixed-layer data, integrating from the bottom of the mixed layer to 110 m. They suggested that including the mixed layer obscures the peak, because the mixed layer becomes deeper north and south of the equator and the dissipation in a mixed layer tends to be larger.

In this paper, a series of datasets are combined to summarize our evidence for and against a peak in turbulence intensity at the equator, coping as best as we can with the temporal variability problem. These datasets include:

1) a transect across the equator in November 1984 from 3°N to 3°S at 140°W,

2) a November 1984 12-day time series on the equator at 140°W,

3) a March 1987 transect from 17°N to 6°S at 140°W,

4) an April 1987 transect from 140°W to 110°W along the equator,

5) an April 1987 transect from 3°S to 6°N along 110°W.

The question of the equatorial peak in turbulence activity originated from the observation that Ri exhibits a local minimum there. It is natural, then, to examine the issues of the Richardson number dependence of ϵ and of the parameterization of turbulence; these issues are discussed with respect to this equatorial data.

2. Experimental methods

The data under consideration were gathered on two R/V *Wecoma* cruises to the equatorial Pacific.

1) During the first cruise, in November 1984 (Chereskin et al. 1986; Moum et al. 1986a; Moum et al. 1989), the winds were moderately strong and relatively constant (westward at 5–10 m s^{-1}). The EUC core at 120 m was strong, approximately 1.5 m s^{-1}, and the surface water flowed westward at approximately 0.3 m s^{-1}.

2) The second cruise consisted of two legs, one from San Francisco to Papeete (mainly along 140°W) and one from Papeete to San Diego (an equatorial transect from 140°W to 110°W and a cross-equatorial transect at 110°W). It took place in the spring of 1987, near the end of the 1986–1987 El Niño (Hebert et al. 1991). Compared to conditions found in 1984, both the surface current and the winds in 1987 were much weaker and more variable, changing direction several times. The EUC core was shallower (100 m) at 140°W than it had been in 1984 and, as expected, shoaled as we moved eastward, to 50 m at 110°W. The EUC was generally weaker in 1987, but increased in speed from 1 m s^{-1} at 140°W to 1.2 m s^{-1} at 110°W.

For both surveys, currents were determined by a 300-kHz acoustic Doppler current profiler (ADCP). The sampling configurations were similar (16-m pulse length and 4-m bin length), although different ADCPs were used. Estimates of the horizontal velocity were made every 4 m vertically starting at a depth of 19.1 m, although independent estimates were obtained approximately every 12 m (Chereskin et al. 1986). In 1987, a problem with the tracking filter of the RDI instrument in regions of large vertical shear (Chereskin et al. 1989) limited the depth of reliable ADCP velocity estimates to 164 m. ADCP data were averaged over one hour.

Profiles of conductivity, temperature, and turbulent velocity shear were made using the RSVP (Caldwell et al. 1985) approximately every 10 minutes; on the transects, this translates to a spacing of approximately one kilometer between profiles. In 1984, line vibration due to the large velocity shear of the equatorial undercurrent limited the depth of reliable dissipation measurements to 110 m, but by 1987 this source of signal contamination had been eliminated. In 1987, the weaker velocity shear, together with a changed configuration of the RSVP profiler, allowed reliable dissipation mea-

surements to deeper depths than in 1984. RSVP data were averaged into the same 4-m depth bins as the ADCP data but starting at a depth of 3.1 m. The RSVP data were also averaged over one hour.

To reduce the effect of temporal variability (due to both the natural intermittency of turbulence and the effects discussed in section 1), further averaging was performed. Since for much of the data the major source of temporal variability was diurnal, the smallest time interval chosen was one day. In depth averaging, two schemes were used.

a. Depth averaging

For comparison with previous work (Crawford 1982; Moum et al. 1986a,b; Peters et al. 1989) we followed Peters et al. (1989) in choosing the depth range 15 m to 110 m over which to compute the "depth-averaged" dissipation rate. This range encompasses the high-shear region above the core of the undercurrent and usually includes both the thermocline and mixed layer. These 15–110 m depth-averaged hourly averaged dissipation rates are denoted by $\bar{\epsilon}$ (Table 1).

Peters et al. (1989) argued that combining data from the surface mixed layer with data from the thermocline would obscure an equatorial peak in ϵ in the high-shear low-Ri thermocline region. They reasoned that the latitudinal variability in mixed-layer depth and the higher contribution to $\bar{\epsilon}$ by the surface mixed-layer dissipation rate could dominate any latitudinal variability in the thermocline dissipation rate when examining the latitudinal variability of $\bar{\epsilon}$. Following Peters et al. (1989), we divided our hourly averaged data into two regions: the surface mixed-layer and the thermocline. The surface mixed-layer region is taken as the region from a depth of 15 m to the mixed-layer depth h_{ml}. We defined the mixed-layer depth as the depth where the density is 0.01 kg m^{-3} larger than the density at 3.1 m. The thermocline region is defined as the region from h_{ml} to a depth of 110 m. For each hourly averaged profile, the average dissipation rate in the surface mixed layer, $\overline{\epsilon_{\mathrm{ml}}}$, and in the thermocline, $\overline{\epsilon_{th}}$, were computed (see Table 1 for a summary of definitions). From values of hourly averaged wind speed, the hourly averaged values of the wind work at 10-m height, E_{10}, were also determined (Large and Pond 1981).

TABLE 1. Summary of notation used in this paper.

1-hour 2-m average turbulent kinetic-energy dissipation rate	ϵ
Mixed-layer depth using 1-hour average density profile	h_{ml}
Wind work at 10-m height using 1-hour average wind speed	E_{10}
Depth-averaged dissipation rate	$\bar{\epsilon}\left(=\frac{1}{(110\text{ m}-15\text{ m})}\int_{15}^{110}\epsilon dz\right)$
Average mixed-layer dissipation rate	$\overline{\epsilon_{\mathrm{ml}}}\left(=\frac{1}{(h_{\mathrm{ml}}-15\text{ m})}\int_{15}^{h_{\mathrm{ml}}}\epsilon dz\right)$
Average thermocline dissipation rate	$\overline{\epsilon_{th}}\left(=\frac{1}{(110\text{ m}-h_{\mathrm{ml}})}\int_{h_{\mathrm{ml}}}^{110}\epsilon dz\right)$
Spatial/temporal average of above quantities (see Table 2 for details)	$\langle\cdot\rangle$
16-m 1-hour average thermocline dissipation rate	ϵ_{th}
16-m 1-hour average buoyancy frequency	N
16-m 1-hour average vertical shear of horizontal currents	S

b. Time averaging

Since some of the data were taken on meridional transects across the equator, some on a zonal transect along the equator and some at a fixed location on the equator, different averaging schemes are appropriate for each. The data can be separated into three groups (Table 2):

1) For the three cross-equatorial transects, one at 140°W in 1984 (84/140°W), one at 140°W in 1987 (87/140°W), and one at 110°W in 1987 (87/110°W), the data were averaged over 2° latitudinal bins and plotted every 0.5° (Fig. 1). Thus, totally independent estimates of the averaged quantities are separated by 2° of latitude. Because the ship speed was approximately 2° day^{-1}, these amount to daily averages.

2) For the data collected during the 12-day time series at 140°W on the equator in 1984 (84TS), all of the data were averaged together and plotted as one point in Figs. 1 and 2, since the hydrographic and wind conditions were relatively constant.

3) For the data taken on the zonal transect along the equator in 1987, 4-day averages (87A, 87B, and 87C) were used because conditions, both meteorological and hydrographic, were approximately constant over each of these periods.

The time-averaged estimates of the quantities $\bar{\epsilon}$, $\overline{\epsilon_{\mathrm{ml}}}$, $\overline{\epsilon_{th}}$, h_{ml}, and E_{10} are represented by $\langle\bar{\epsilon}\rangle$, $\langle\overline{\epsilon_{\mathrm{ml}}}\rangle$, $\langle\overline{\epsilon_{th}}\rangle$, $\langle h_{\mathrm{ml}}\rangle$, and $\langle E_{10}\rangle$.

3. Meridional variability

Is there an enhanced mean dissipation rate at the equator, where the mean Richardson number above the EUC is small, compared to that found in the regions north and south of the equator where the mean Richardson number is generally higher?

For two of the three cross-equatorial transects (87/140°W and 87/110°W), the spatially (temporally) averaged depth-integrated dissipation rate $\langle\bar{\epsilon}\rangle$ showed a peak in $\langle\bar{\epsilon}\rangle$ at the equator (Fig. 1). Although there

TABLE 2. Description of the different datasets used in the analysis, the averaging used to eliminate any diurnal variability, and the number of hourly samples used in each $\langle \cdot \rangle$ average.

Date	Location	Abbreviation	$\langle \cdot \rangle$	Number of samples
15–18 Nov 1984	3°N–3°S 140°W	84/140°W	2° of latitude (approx. daily)	24
19 Nov–1 Dec 1984	Equator 140°W	84TS	12 days	288
13–27 Mar 1987	17°N–6°S 140°W	87/140°W	2° of latitude (approx. daily)	24
14–18 Apr 1987	Equator 140°W–132°W	87A	4 days (8° of longitude)	96
19–23 Apr 1987	Equator 130°W–121°W	87B	4 days (9° of longitude)	96
24–28 Apr 1987	Equator 119°W–110°W	87C	4 days (9° of longitude)	96
1–5 May 1987	3°S–6°N 110°W	87/110°W	2° of latitude (approx. daily)	24

was no evidence of a peak in $\langle \bar{\epsilon} \rangle$ for transect 84/140°W, an increase in $\langle \overline{\epsilon_{th}} \rangle$, the thermocline dissipation, at the equator was observed, although it was not significant at the 95% level. In this case, the high dissipation rate in the mixed layer, the depth of which varied diurnally and latitudinally (Fig. 1d), concealed the latitudinal variability of ϵ_{th}. Also, transect 84/140°W did not extend far from the equatorial undercurrent [see Fig. 1c of Moum et al. (1986a) and Fig. 1d]; data from regions of high shear have been averaged into $\langle \overline{\epsilon_{th}} \rangle$, even at the ends of the transect. The variability in $\langle \overline{\epsilon_{th}} \rangle$ is very similar to $\langle \bar{\epsilon} \rangle$ near the equator, partially because $h_{ml} \sim 15$ m (that is, the limits of integration are very similar).

There was significant longitudinal and temporal variability in $\langle \bar{\epsilon} \rangle$ (and $\langle \overline{\epsilon_{th}} \rangle$) as well as latitudinal variability (Fig. 1). It is likely that the past history of wind forcing played some role in the level of $\langle \overline{\epsilon_{th}} \rangle$. For example, $\langle \overline{\epsilon_{th}} \rangle$ for the long station, 84TS, made a few days after transect 84/140°W, was smaller than all $\langle \overline{\epsilon_{th}} \rangle$ found for transect 84/140°W. However, the average wind work for 84TS was larger than $\langle E_{10} \rangle$ south of 1°N during 84/140°W. During transect 84/140°W, the wind work south of the equator was half of that at the northern end, the start of the transect. After 84/140°W, the mean wind work increased slightly for the period of 84TS, although the winds were weaker for the first three days of 84TS (Moum et al. 1989). Also, short strong wind events can produce off-equatorial peaks in the dissipation rate. During 87/140°W, the peak in $\langle \overline{\epsilon_{th}} \rangle$ occurred at 1°N; this peak was dominated by large dissipation rates from one large wind event observed on 22 March, while the ship occupied a position near 1°N for a day (Hebert et al. 1991). Removal of the data from this one day would reduce the $\langle \overline{\epsilon_{th}} \rangle$ shown in Fig. 1 to the level found for 84/140°W, and the new peak in $\langle \overline{\epsilon_{th}} \rangle$ would be skewed more toward the equator. This temporal variability in the wind work makes the determination of the spatial variability difficult.

Although changes in $\langle \overline{\epsilon_{th}} \rangle$ are associated with changes in the wind work (Fig. 2), this effect did not completely obscure the peak in $\langle \overline{\epsilon_{th}} \rangle$ at the equator for the transects (Fig. 1). Away from the EUC (i.e., locations greater than 3° from the equator), $\langle \overline{\epsilon_{th}} \rangle$ values were smaller than $\langle \overline{\epsilon_{th}} \rangle$ values on the equator for the same wind work (Fig. 2). Temporal variability in wind work could produce a fictitious peak in $\langle \overline{\epsilon_{th}} \rangle$; if the wind speed is a factor of 3 larger off the equator than that found on the equator, any peak in $\langle \overline{\epsilon_{th}} \rangle$ at the equator would be obscured (Fig. 2). Therefore, it is necessary to examine the variability in the wind field when comparing dissipation measurements.

The mixed layer was shallow (<15 m) for most of the data collected (Fig. 1d); thus, there was little data available for examining the variability of $\overline{\epsilon_{ml}}$. The sample sizes were such that confidence limits only for station 84TS, the off-equatorial parts of transect 84/140°W, parts of 87/140°W, 87A, and 87C could be determined. Therefore, we will not examine the variability of $\overline{\epsilon_{ml}}$ or determine whether $\overline{\epsilon_{ml}}$ was enhanced above the dissipation rate based on similarity scaling, as found by Peters et al. (1989).

Into $\overline{\epsilon_{th}}$ has gone ϵ values from a wide range of stratification and velocity shear. To examine ϵ as a function of Ri below the mixed layer, it would be improper to compare $\overline{\epsilon_{th}}$ with estimates of average N^2, S^2, and Ri in the thermocline based on the mean vertical gradients of velocity and density over the same depth range used for determining $\overline{\epsilon_{th}}$. The variation of S is too large;

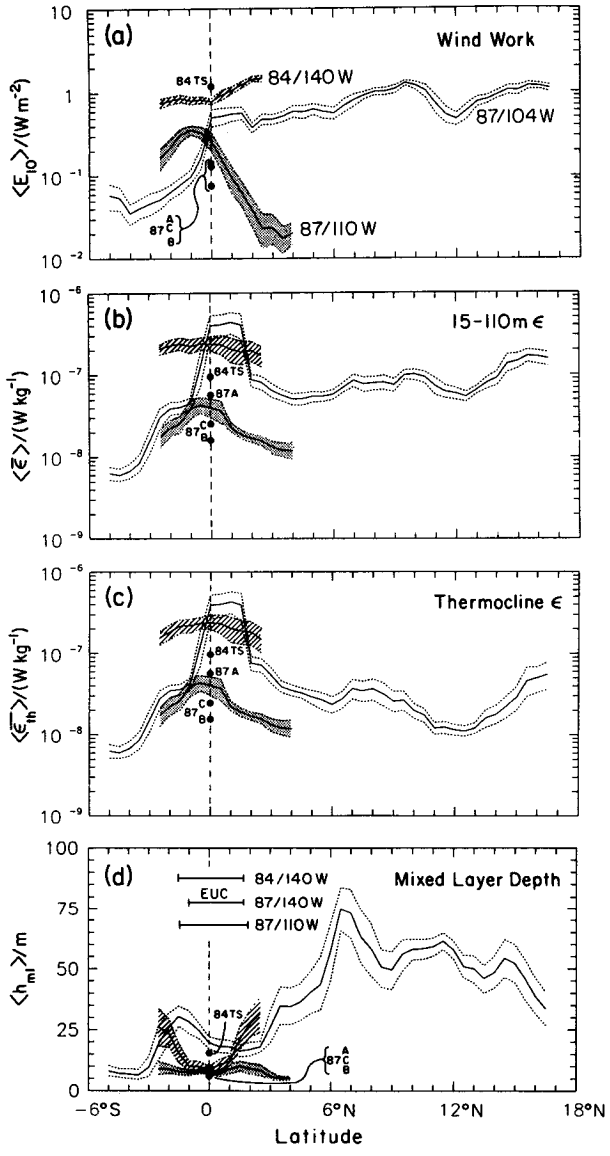

FIG. 1. Averaged (see Table 2 for details) (a) wind work at 10-m height, (b) depth-averaged dissipation rate, (c) average thermocline dissipation rate, and (d) mixed layer depth for the different datasets, as a function of latitude. The 95% confidence limits on the mean, obtained by the bootstrap method (Efron and Gong 1983), are shown. The 95% confidence limits for 84/140°W and 87/110°W have been shaded. Approximate width of the EUC (region where the velocity at the depth of core > 0.25 m s^{-1}) for the three cross-equatorial transects is shown in (d).

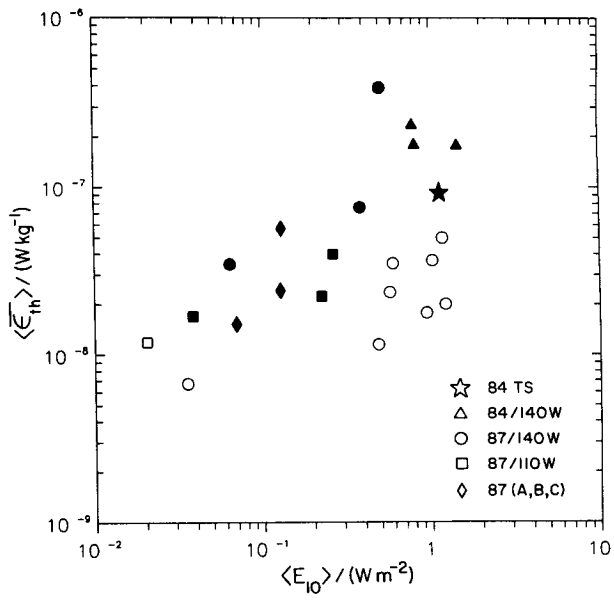

FIG. 2. Dissipation rate $\langle \overline{\epsilon_{th}} \rangle$ as a function of $\langle E_{10} \rangle$ for the different datasets. For the cross-equatorial transects, only data from even degrees of latitude are used. Thus, they are independent estimates. For locations on the equator (i.e., less than 3° away from the equator), the symbols have been filled.

regions such as 110°W, where the EUC is located at a depth of 50 m, would give S^2 of nearly zero using the average vertical gradient of horizontal velocity over the thermocline (defined earlier as the depth range h_{ml} to 110 m), while S^2 above the core of the EUC was approximately 5×10^{-4} s^{-2}. Therefore, in the next section we examine the dependence of the dissipation rate in the thermocline, ϵ_{th}, on N^2 and S^2 at the smallest temporal and spatial scales for which N^2 and S^2 can be determined reliably.

4. Richardson number dependence

Is mixing enhanced (and dissipation rates higher) when the Richardson number is smaller?

In determining the Richardson number in these datasets, the vertical shear in the horizontal velocity was obtained from the ADCP. This places constraints on the vertical scale of shear that can be resolved. With this limitation, it was decided to determine the vertical shear and density gradient over 16 m every 8 m from the hourly averaged data. [With a vertical pulse length of 16 m and bin length of 4 m (used in both 1984 and 1987), vertical shear with a wavelength of 20 m is attenuated by a factor of 5, and shear with a wavelength of 50 m is reduced by a factor of 1.2.] The hourly average dissipation for each 16-m region was also determined. This 16-m hourly averaged data was used for the following analyses.

If ϵ_{th} is contoured in N^2–S^2 space, using all the data from between h_{ml} and 110 m for both the 1984 and 1987 surveys, it is apparent that ϵ_{th} increased as Ri decreased below 1 (Fig. 3). (In Fig. 3, lines of constant Ri have a slope of +1.) For Ri $\leq$ 1, contours of ϵ are approximately parallel to constant Ri lines, implying that ϵ_{th} depends simply on Ri. [Even with over 12 000 data points (hourly averaged 16-m depth averaged),

only two decades of N^2 and S^2 in the low-Ri regime have a sufficient number of ϵ values to get a good estimate of the mean ϵ_{th}. To get more data in the lower N^2 regime, it will be necessary to profile deeper.] For Ri $\gg$ 1, the dependence of ϵ_{th} on Ri is less clear. Although there still appears to be a Ri dependence, for the region ($S^2 < 10^{-5}$ s^{-2}, Ri > 10), the mean ϵ_{th} appeared to decrease with decreasing shear and to be independent of N^2. Separating the thermocline data into two groups, on-equatorial (within 3° of the equator) and off-equatorial, we found no significant difference in trends between the two groups, the principal difference being the dearth of Ri < 1 values for the off-equatorial group.

The presence of low average (hourly, 16-m vertical) Ri in a given location does not necessarily mean that the dissipation rate is always high. Moum et al. (1989) showed a similar situation where the 1-hour 24-m average dissipation rate varied by more than 3 orders of magnitude even though Ri remained approximately 0.2. From observations in 1984, it was speculated that the high dissipation rates observed below h_{ml} on the equator were due in part to high-frequency internal waves. The ADCP cannot resolve the vertical shear of the high-frequency, short horizontal wavelength (~150 m) internal waves (Moum et al. 1991). Therefore, any ϵ dependence on N^2, S^2, and Ri observed in Fig. 3 is valid only for the mean and not for each ϵ estimate.

5. Consequences for mixing parameterizations

It has been speculated that the eddy coefficients for mass (K_ρ) and momentum (K_m) can be parameterized in terms of the background stratification and/or shear (e.g., McCreary 1981; Gargett and Holloway 1984; Peters et al. 1988; Gregg 1989; Gargett 1990). Most of these parameterizations are based on internal wave dynamics with ϵ due to wave "breaking" and no mean

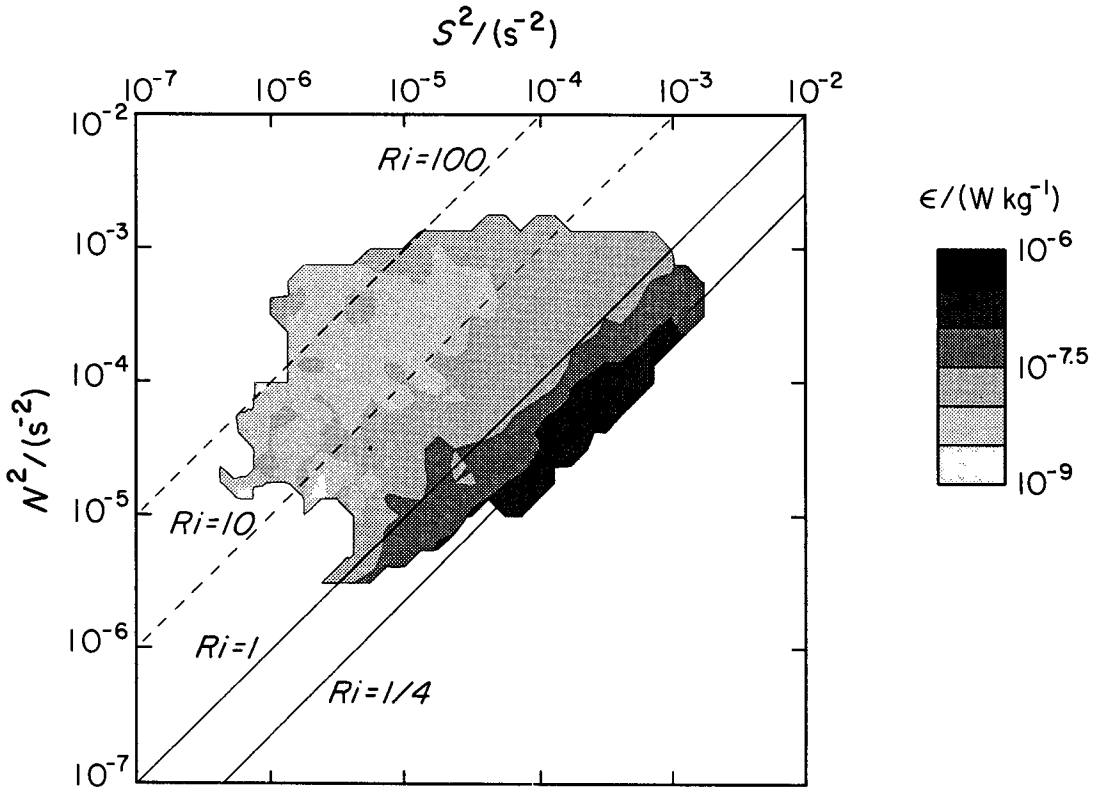

FIG. 3. Average (1-h 16-m) thermocline dissipation rate, ϵ_{th}, as a function of average (1-h 16-m) velocity shear, S^2, and stratification, N^2, for all of the 1984 and 1987 data. Constant lines of Ri = 0.25, 1, 10, and 100 are shown. The mean ϵ at each grid point, on the 41 × 41 grid with uniform spacing in log(N^2) and log(S^2), was a weighted average of all ϵ values within one grid spacing (0.125) of the gridpoint location, with the weights decreasing linearly from 1 if the data point coincided with the gridpoint location, to 0 if the data point was one grid spacing away from the gridpoint location. Only gridpoint locations with 10 or more points used in determining the mean ϵ at the grid point were used in the contouring. Given the large dynamic range of mean ϵ over the (N^2, S^2) domain, log(ϵ) was contoured. For almost all of the contoured region, the 95% confidence limits on the mean ϵ (based on the bootstrap method) were less than 0.5 in log(ϵ). It should be noted that, for the bootstrap method to give a proper estimate of the confidence limits, the sample population must adequately represent the true population distribution.

background shear present (i.e., the critical Richardson number is based on the internal wave shear). With the low mean Ri in the equatorial Pacific, it has been suggested that the eddy coefficients are simple functions of mean N^2 (McCreary 1981) or mean Ri (Pacanowski and Philander 1981; Peters et al. 1988) for this region. Unfortunately, there are no physical models for justification of these parameterizations of mixing for the equatorial ocean like the models for the parameterizations of mixing by breaking internal waves.

Estimates of the turbulent vertical fluxes of momentum and mass can be obtained from measurements of the dissipation rate. Details of the assumptions made for obtaining vertical fluxes by this method are reviewed by Gregg (1987). Using these standard turbulence relationships for the eddy coefficients K_m and K_ρ,

$$\epsilon \propto K_m S^2, \quad \epsilon \propto K_\rho N^2 \tag{1}$$

we see that if

$$K_\rho \propto \mathrm{Ri}^{-n} \tag{2}$$

(Peters et al. 1988) then

$$\epsilon \propto N^2 \mathrm{Ri}^{-n}; \tag{3}$$

therefore, ϵ is not a function of Ri only. Also, it follows from (1) and (3) that

$$K_m \propto \mathrm{Ri}^{1-n}. \tag{4}$$

From comparing K_ρ (based on the dissipation data) to Ri, Peters et al. (1988) found that n was 9.2. If this relationship between K_ρ and Ri is true, then constant ϵ lines in Fig. 3 would have a slope of 1.1 instead of a slope of 1 for a dependence on Ri alone. We cannot distinguish between a slope of 1 and 1.1 for constant ϵ contours in Fig. 3. However, the 95% confidence limits on Peters et al.'s (1988) estimate of n were ± 4.0. If n were 5.2 instead, constant ϵ lines in Fig. 3 would have a slope of 1.2, which is significantly different from what is observed. We believe that the predicted slope of constant ϵ lines for n less than 7.7 (i.e., a slope greater than 1.15) could be distinguished from the observed slope of 1 in Fig. 3. Therefore, either $K_\rho \propto \mathrm{Ri}^{-n}$ and $\epsilon \propto N^2\,\mathrm{Ri}^{-n}$ with $n > 7.7$ or K_ρ depends on N^2 as well as Ri and $\epsilon = \epsilon(\mathrm{Ri})$ only.

The structure of $\epsilon(N^2, S^2)$ is more complicated if the eddy coefficient for momentum is of the form

$$K_m = K_m{}^b + \frac{K_m{}^0}{(1 + 5\mathrm{Ri})^2} \tag{5}$$

where $K_m{}^b$ and $K_m{}^0$ are constants, as suggested by Pacanowski and Philander (1981). Based on their dissipation measurements, Peters et al. (1988) suggested that the exponent on the denominator in (5) be 1.5 instead of 2 and that this parameterization is only for $\mathrm{Ri} > 0.4$. For the parameterization of K_m in (5), and using (1), constant ϵ curves would have a slope of approximately 2 in the $\mathrm{Ri} \approx 1$ region. This is definitely not true for our data (Fig. 3). Interestingly, (5) predicts that $K_m \approx K_m{}^b$ (a constant) for $\mathrm{Ri} \gg 1$. This implies that ϵ is independent of N^2 in this region (and depending only on S^2), as speculated earlier from our data (Fig. 3). Although the functional form of (5) was determined empirically and has the appropriate characteristics of the observed ϵ at high Ri, there is no physical justification for this parameterization.

Although ϵ appears to depend on Ri, the true dependence of ϵ might be related to some other parameter with which Ri is highly correlated. For example, in the equatorial Pacific region, Ri increases with increasing depth until the core of the EUC is reached before it begins to decrease again. Peters et al. (1988) suggested that their observed Ri dependence of ϵ could have been due to just a depth dependence of ϵ. In the 1984 and 1987 TROPIC HEAT data, there was a definite depth dependence of ϵ (Fig. 4), even for a constant Ri. Similar depth variability of K_ρ and K_m for constant Ri was also found. This implies that the depth variability observed is not just a N^2 or S^2 dependence and that K_ρ and K_m are not just functions of Ri. Any $\epsilon(\mathrm{Ri})$ [or $K_\rho(\mathrm{Ri})$ and $K_m(\mathrm{Ri})$] fit to the data would have to be different for different depths. It is obvious that a simple parameterization of ϵ (or K_ρ and K_m) on Ri must have coefficients that are depth dependent. It is not appropriate to use (2), (4), or (5) with coefficients that are depth independent as given by Pacanowski and Philander (1981) or Peters et al. (1988).

6. Discussion

In looking for a peak in the dissipation rate at the equator, it is assumed that either the high shear or low Richardson number plays a role in the amount of turbulence present, either as simple shear-driven turbulence or as a precondition for other instabilities to occur. In determining the average thermocline dissipation rate, ϵ values from a wide range of stratification and shear have been averaged to produce one average thermocline dissipation rate. Using all of our thermocline dissipation rates collected within 17° of the equator, we found that the mean ϵ_{th}, when grouped in (N^2, S^2) space, appeared to be a function of only the Richardson number when $\mathrm{Ri} < 1$. For $\mathrm{Ri} > 1$, there was no obvious dependence of ϵ_{th} on Ri. Sorting the data into the two years (1984 and 1987), which is almost equivalent to sorting the data into high and low winds regimes, we found the same result as the combined dataset except that the 1984 dissipation rates were slightly larger than the 1987 dissipation rates for the same N^2 and S^2.

The association of higher mean dissipation rates with smaller mean Ri for $\mathrm{Ri} < 1$, found when all of the data were combined, does not imply that for small Ri all ϵ_{th} values were large. Moum et al. (1991) examined the temperature fluctuations on time scales of 10 s to 300

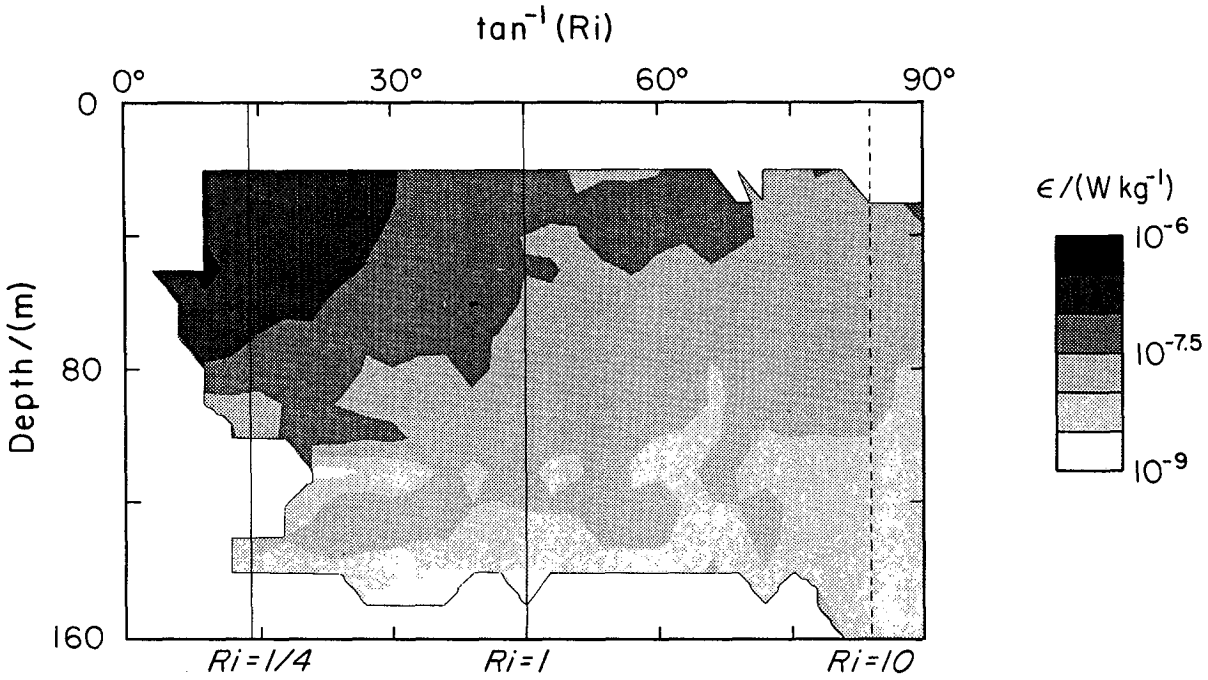

FIG. 4. Dissipation rate ϵ_{th} as a function of depth and Ri. The contour plot is based on a 31 × 17 grid, spaced equally in $\tan^{-1}$ (Ri) and depth, using the same procedure as described in Fig. 3.

s from the towed thermistor chain (equivalently, horizontal scales of 25 m to 750 m since horizontal changes in temperature field cannot be separated from temporal changes) during the 1987 equatorial transect. They found the hourly averaged ϵ values to be highly correlated with the hourly rms temperature fluctuations believed to be due to high-frequency internal waves. Moum et al. (1991) showed that the vertical shear by the high-frequency internal waves has a depth dependence with the largest wave shears occurring near the surface. This wave shear will preferentially reduce the instantaneous Ri near the surface and could explain the observed ϵ(Ri, z) dependence (Fig. 4).

The presence of these waves seems to be necessary to have high dissipation for the low-Ri number region in the equatorial Pacific. These internal waves were present during 87A but not during 87B or 87C. The presence of these waves appears to be correlated to the strength of the winds; few or no waves were observed when the winds were low. Thus, the high dissipation rates in the thermocline are not due to just the low Ri conditions but to the presence of other features, such as high-frequency internal waves, which act in concert with the low Ri mean conditions found at the equator.

Attempts have been made to represent eddy coefficients for mixing in the equatorial Pacific in terms of the mean Ri (Pacanowski and Philander 1981; Peters et al. 1988). Although for the Ri < 1 region ϵ_{th} appears to depend on Ri, we found that there was also a depth dependence of ϵ_{th} independent of Ri. Parameterizing mixing coefficients only in terms of Ri would be improper. However, with the data collected at the equator to date, only during the latter half of the equatorial transect in 1987 was ϵ measured consistently in the high shear region below the undercurrent. Unfortunately, there were none of the high-frequency internal waves believed necessary for the high ϵ values present during this period. To explicitly separate the effect of the surface forcing (i.e., E_{10}) and/or small-scale forcing (i.e., internal waves) from the influence of Ri on the mean dissipation rate, it would be necessary to sample ϵ in two regions of a similar low mean Ri at the same time (i.e., above and below the undercurrent).

7. Conclusions

On the basis of more than 8000 microstructure casts taken on cruises to the eastern equatorial Pacific, we conclude the following:

- The natural variability in dissipation on the time scale necessary for a cross-equatorial transect obscures the question of the enhancement of dissipation over the EUC. The sources of variability on time scales of a few days or less are:

1) The natural intermittency of turbulence, in this case possibly compounded with variability caused by internal waves.
2) The diurnal cycle of the vertical buoyancy flux,

which appears to cause a strong diurnal variability in turbulence when winds are high.

3) Changes in the local wind speed.

Other sources of variability on these time scales and others may well be present also. An unresolved factor is the history of the wind field. The mechanism by which the wind induces the mixing in the thermocline is unknown. Therefore, we cannot determine how much of the past history of the wind affects the observed dissipation rates.

- The dissipation is enhanced above the core of the EUC, relative to the same depths at latitudes to the north and south.
- The dissipation depends more on the Richardson number than it does on the shear or the stratification considered alone.
- The dependence on the Richardson number is not unique, even in this restricted depth range. In particular, the dependence of dissipation on the Richardson number changes with depth. The use of formulas prescribing dissipation in terms of the Richardson number only is not justified.

The Richardson number used in this discussion is a highly averaged estimate, averaged over both time and space. The estimate for shear used in its calculation has the inherent spatial averaging of the ADCP, whereas the stratification and dissipation are measured along the path of the descending RSVP. With all the averaging that we did, our estimates of the Richardson number became more similar to those used in large-scale model calculations than to local values envisioned in the usual fluid mechanics concept.

Acknowledgments. This work was funded by the National Science Foundation (Grants OCE-8214639, OCE-8608256, and OCE-8716719).

REFERENCES

Caldwell, D. R., T. M. Dillon and J. N. Moum, 1985: The Rapid Sampling Vertical Profiler—An evaluation. *J. Atmos. Oceanic. Technol.*, **2,** 615–625.

Chereskin, T. K., E. Firing and J. A. Gast, 1989: Identifying and screening filter skew and noise bias in acoustic Doppler current profiler measurements. *J. Atmos. Oceanic Technol.*, **6,** 1040–1054.

——, J. N. Moum, P. J. Stabeno, D. R. Caldwell, C. A. Paulson, L. A. Regier and D. Halpern, 1986: Fine-scale variability at 140°W in the equatorial Pacific. *J. Geophys. Res.*, **91,** 12 887–12 897.

Crawford, W. R., 1982: Pacific equatorial turbulence. *J. Phys. Oceanogr.*, **12,** 1137–1149.

——, and T. R. Osborn, 1981: Control of equatorial ocean currents by turbulent dissipation. *Science,* **212,** 539–540.

Efron, B., and G. Gong, 1983: A leisurely look at the bootstrap, the jackknife, and cross-validation. *Am. Stat.*, **37,** 36–48.

Gargett, A. E., 1990: Do we really know how to scale the turbulent kinetic energy dissipation rate ϵ due to breaking of oceanic internal waves? *J. Geophys. Res.*, **95,** 15 791–15 974.

——, and G. Holloway, 1984: Dissipation and diffusion by internal wave breaking. *J. Mar. Res.*, **42,** 14–27.

Gregg, M. C., 1987: Diapycnal mixing in the thermocline: A review. *J. Geophys. Res.*, **92,** 5249–5286.

——, 1989: Scaling turbulent dissipation in the thermocline. *J. Geophys. Res.*, **94,** 9686–9698.

——, H. Peters, J. C. Wesson, N. S. Oakey and T. S. Shay, 1985: Intensive measurements of turbulence and shear in the equatorial undercurrent. *Nature,* **318,** 140–144.

Hebert, D., J. N. Moum, C. A. Paulson, D. R. Caldwell, T. K. Chereskin and M. J. McPhaden, 1991: The role of the turbulent stress divergence in the equatorial Pacific zonal momentum balance. *J. Geophys. Res.*, **96,** 7127–7136.

Large, W. G., and S. Pond, 1981: Open ocean momentum flux measurements in moderate to strong winds. *J. Phys. Oceanogr.*, **11,** 324–336.

McCreary, J. P., 1981: A linear, stratified ocean model of the equatorial undercurrent. *Phil. Trans. R. Soc. London,* **A298,** 603–635.

Moum, J. N., and D. R. Caldwell, 1985: Local influences on shear-flow turbulence in the equatorial ocean. *Science,* **230,** 315–316.

——, D. R. Caldwell, C. A. Paulson, T. K. Chereskin and L. A. Regier, 1986a: Does ocean turbulence peak at the equator? *J. Phys. Oceanogr.*, **16,** 1991–1994.

——, T. R. Osborn and W. R. Crawford, 1986b: Pacific equatorial turbulence: Revisited. *J. Phys. Oceanogr.*, **16,** 1516–1522.

——, D. R. Caldwell and C. A. Paulson, 1989: Mixing in the equatorial surface layer and thermocline. *J. Geophys. Res.*, **94,** 2005–2021.

——, D. Hebert, C. A. Paulson and D. R. Caldwell, 1991: Turbulence and internal waves at the equator. Part I: Statistics. *J. Phys. Oceanogr.*, submitted.

Pacanowski, R. C., and S. G. H. Philander, 1981: Parameterization of vertical mixing in numerical models of tropical oceans. *J. Phys. Oceanogr.*, **11,** 1443–1451.

Peters, H., M. C. Gregg and J. M. Toole, 1988: On the parameterization of equatorial turbulence. *J. Geophys. Res.*, **93,** 1199–1218.

——, —— and ——, 1989: Meridional variability of turbulence through the equatorial undercurrent. *J. Geophys. Res.*, **94,** 18 003–18 010.

Turner, J. S., 1973: *Buoyancy Effects in Fluids.* Cambridge University Press, 368 pp.